Journal of Applied Polymer Science

Comparative Study on the Crystallization Behavior of β-isotactic Polypropylene Nucleated with Different β-nucleation Agents —Effects of Thermal Conditions

Jian Kang, Hongmei Peng, Bin Wang, Zhengfang Chen, Jingping Li, Jinyao Chen, Ya Cao, Huilin Li, Feng Yang, Ming Xiang

State Key Laboratory of Polymer Materials Engineering, Polymer Research Institute of Sichuan University, Chengdu 610065, People's Republic of China

Correspondence to: F. Yang (E-mail: yangfengscu@126.com) or M. Xiang (E-mail: xiangming45@hotmail.com)

ABSTRACT: In this study, the crystallization behavior of the β-isotactic polypropylene (β-iPP) samples nucleated by a rare earth based β-nucleating agent (β-NA) WBG-II and a metal salts compound β-NA NAB83 (denoted as WPP and NPP, respectively) under different cooling conditions were comparatively investigated. The thermal conditions such as the cooling rate, isothermal crystallization temperature, isothermal crystallization time, and the subsequent cooling to room temperature. The results of WAXD, SEM, and nonisothermal crystallization reveal that under the same processing conditions, the crystallite size of NPP is smaller, which arrange more compactly as compared with WPP. Meanwhile, NPP has shorter crystallization rate and higher β-nucleation selectivity, but WPP can crystallization at wider temperature range. The results of isothermal crystallization showed that NPP has higher selectivity and higher β-nucleation efficiency, which favors the formation of high proportion of β-phase at the isothermal crystallization temperature of 110–130°C with and without subsequent cooling; WPP has lower selectivity, which can only induce high content of β-phase under isothermal crystallization without subsequent cooling to 25°C. In tuning the crystallization behavior and the properties of β-PP, the joint influence of the efficiency and selectivity of the β-NA, and the thermal conditions should be taken into consideration.
 J. Appl. Polym. Sci. **2014**, *131*, 40115.

KEYWORDS: crystallization; polyolefins; thermal properties

Received 8 July 2013; accepted 24 September 2013
DOI: 10.1002/app.40115

INTRODUCTION

Isotactic Polypropylene (iPP) is a kind of widely used commodity polymer, which has relative low manufacturing cost and rather versatile properties.[1–5] iPP exhibits a very interesting polymorphic behavior, depending on the molecular structure,[6] thermal history,[7] and the presence of external materials.[8,9] Three types of crystalline structures of iPP are known, including the monoclinic α-form,[10] the trigonal β-form,[11–14] and the triclinic γ-form.[15–17] Among these crystalline structures, β-form has many advantages such as improved ductility and impact strength, and receives great attention in the past years. It is found that the β-form is metastable and difficult to obtain under normal processing conditions. A higher proportion of the β-form can be achieved only by melt crystallization in the presence of certain heterogeneous nucleating agents, by directional crystallization in certain temperature gradients, or from melts subject to shear.[18] Among these the addition of β-nucleating agent (β-NA) is an effective and practical way to obtain or increase the β-fraction, which is the most commonly used way to produce β-PP.

When compared with diverse α-nucleating agents, β-NAs usually have higher selectivity, and there are until now only several classes of compounds have been mainly used as β-NAs[19]: the first class consists of a minority of aromatic ring compounds; the second class includes certain group IIA metal salts or their mixtures with some specific dicarboxylic acids; and the third class is some substituted aromatic bisamide. Actually, the different types of β-NAs usually exhibit different nucleation efficiencies and selectivities. A typical dual-selective β-nucleating agent is the rare earth based β-NA (tradename WBG-II). Besides its high nucleation efficiency,[20] it also exhibits the dual-selectivity,[21] which enhances both α- and β-form in iPP. Moreover, it exhibits the self-organization behavior depending on the thermal conditions applied. Luo et al.[22] argued that the fusion temperature (T_f) determines its solubility of in PP, and thus influences its self-organization behavior, resulting in different

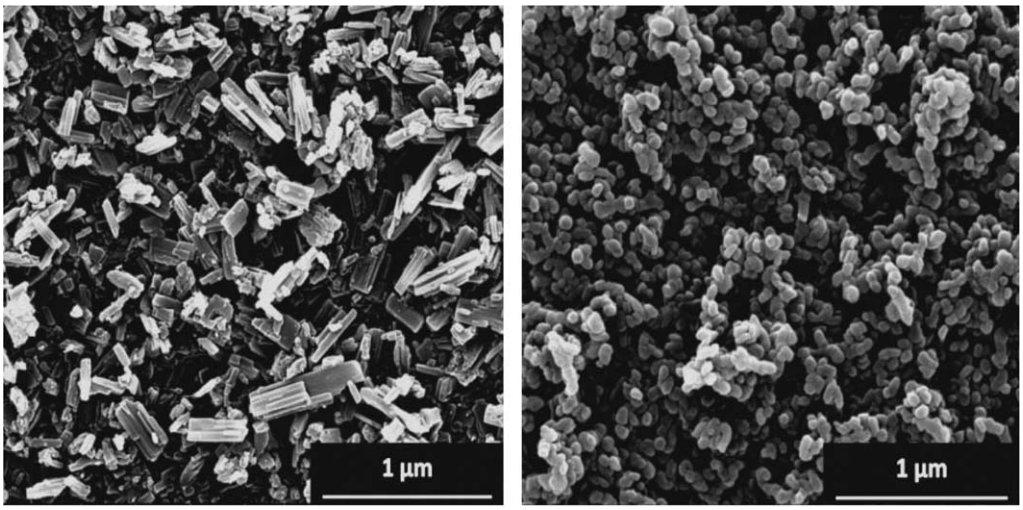

Figure 1. SEM micrograph of the β-nucleating agents (a) WBG-II and (b) NAB83.

supermolecular structures and toughness performances of the β-iPP. On the other hand, some β-NAs possess higher selectivity and can only induce the formation of β-phase. A representative example is the group metal salts based β-NA (such as the metal carboxylate of tetrahydrophthalic anhydride), which is usually used in the production of fibril and membranes to induce the formation of high proportion of β-crystal.[23] However, up to date, the action mechanism of these β-NAs are still not clear; the similarities and differences in the performance, efficiency, and mechanism of the various β-NAs are still ambiguous and need to be further understood. Therefore, to comparatively study the performance and their dependences on the processing conditions (such as thermal and mechanical conditions) of different β-NAs is of importance, since it can not only provide detailed information and differences between the β-NAs, but also help us to deeply understand their fundamental mechanisms.

On the other hand, the researchers claimed that in the production of β-PP, the thermal conditions such as cooling rate, isothermal crystallization, and the lower cooling temperature are important factors in determining the crystallization, morphology, and final properties of β-PP,[7,24–30] especially in the applications, which is greatly dependent on the crystallization behavior and morphology of the sample,[31,32] such as the production of β-microporous membranes.[33,34] Plenty of works have focused on this area, and great progress has achieved.[35–38] However, the understanding of the crystallization behavior of β-PP under the combination influence of β-NA and thermal conditions are still not clear enough, which is of great importance in tuning the crystallization and properties of β-PP.

In this article, a rare earth based β-NA (WBG-II) and a metal salts based β-NA (NAB83) were comparatively investigated on their nucleating efficiencies under different thermal conditions, as well as the subsequent melting behavior of the β-PP, in order to provide new understanding in the relationship between β-NA, thermal conditions and the crystallization behavior of β-PP.

EXPERIMENTAL

Materials

iPP, Trade name T38, polymerized by Lanzhou OilChem with an average isotacticity 97.6%, weight molecular weight $M_w = 34{,}7200$, polydispersity index (PDI) = 3.63, melt index (MI) = 3.0 g/10 min (2.16 kg, 230°C) was used in this study.

Two types of β-NAs, WBG-II, and NAB83, were supplied by Guangdong Winner Functional Materials (PR China) and Guangzhou Chenghe (GCH) technology company (PR China), respectively. WBG-II is heteronuclear dimetal complex of lanthanum and calcium with some specific ligands, which is a kind of irregular block-like crystal whose single crystal diameters is about 10s of nanometers as shown in Figure 1(a). The WBG-II has a general formula of $Ca_xLa_{1-x}(LIG1)_m(LIG2)_n$, where x and $1 - x$ is the proportion of Ca^{2+} and La^{3+} ion in the complex, while LIG1 and LIG2 are respectively a dicarboxylic acid and amide-type ligand with coordination numbers of m and n.

NAB83 is a powder of metal carboxylate of tetrahydrophthalic anhydride, which is a kind of granulates with the diameter of 10s of nanometers [Figure 1(b)]. Its general formula is shown in Figure 2. In Figure 2, the substituent groups of R_1, R_2, R_3, R_4, R_5, R_6, R_7, and R_8 are independently selected from: hydrogen, C1—C9 alkyl group, hydroxyl, phenyl group, and halogen, while M is metal cation selected from barium, calcium, magnesium, strontium, and zinc.

Sample Preparation

The iPP pellets and the β-NAs were mixed in the weight ratio of 100:1 and then extruded by a twin-screw extruder (SHJ-20, Nanjing Giant Machinery, the screw speed is 10 rpm and the temperature of each part is 185, 195, 200, 200°C, respectively) and pelletized to obtain a master batch. The master batch and iPP were mixed and extruded by twin-screw again to obtain β-iPP pellets. The concentration of nucleating agent was 0.2 wt %. The obtained β-iPP samples nucleated with NAB83 and WBG-II were named as NPP and WPP, respectively.

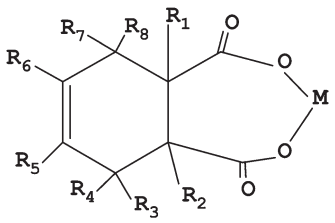

Figure 2. The general formula of NAB83.

For the wide-angle X-ray diffraction (WAXD) and scanning electronic microscopy (SEM) measurements, the thin-sheet samples were prepared. The virgin polymers were molded at 210°C, 10 MPa for 5 min into thin sheets of 500 μm thickness, and then cooled down at the molding temperature of 30°C and molding pressure of 10 MPa.

Characterization

Differential Scanning Calorimetry (DSC). All the calorimetric experiments were performed with Mettler Toledo DSC1 differential scanning calorimeter (DSC) under nitrogen atmosphere (50 mL/min). The temperature scale calibration was performed using indium as a standard to ensure reliability of the data obtained. To ensure the homogeneity of samples and the good contact between sample and pan, the virgin polymer was molded at 190°C, 10 MPa for 5 min into sheets of uniform thickness about 500 μm. Then 5 mg round samples were punched out of the sheets.

All the thermograms were fitted using Peakfit 4.12 software according to the manner in Ref. 7. The relative percentage crystallinities of α-crystal (α_c) and β-crystal (β_c) were estimated from DSC by the following expressions:

$$\alpha_c = X_\alpha/(X_\beta + X_\alpha) \quad (1)$$

$$\beta_c = X_\beta/(X_\beta + X_\alpha) \quad (2)$$

where the degree of crystallinities X associated with each phase, X_α and X_β were calculated from the ratio $\triangle H/\triangle Hu$. $\triangle H$ and $\triangle Hu$ are the apparent and completely crystalline heats of fusion, respectively, and the values used for $\triangle Hu$ for 100% crystalline iPP, was 209 J/g.[8,39]

Scanning Electronic Microscopy. A JSM-5900 LV environmental SEM was used at an accelerating voltage of 20 kV. Before SEM characterizations, the surfaces of all the samples were coated with a thin layer of gold by ion sputtering. On the other hand, for characterizing the crystallization structure of the samples, all the samples were etched for 2 h in a solution containing 1.3 wt % potassium permanganate (KM_nO_4), 32.9 wt % concentrated sulfuric acid (H_2SO_4), and 65.8 wt % concentrated phosphoric acid (H_3PO_4), according to the procedure proposed by Olley et al.[40]

Wide-Angle X-ray Diffraction. WAXD patterns were recorded with a DX-1000 diffractometer. The X-ray wavelength of CuKα radiation was $\lambda = 0.154$ nm and the spectra were recorded in the 2θ range of 5°–35°, a scanning rate of 2°/min, and a scanning step of 0.02°. The crystallite size L of each plane of samples was determined from the XRD using the Debye–Scherrer's equation[8,41]:

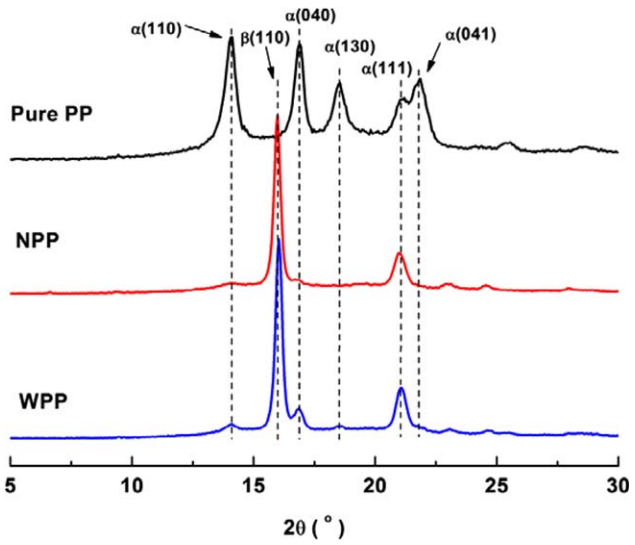

Figure 3. WAXD profiles of pure PP, NPP, and WPP. [Color figure can be viewed in the online issue, which is available at wileyonlinelibrary.com.]

$$L = 0.9\lambda/\beta\cos\theta \quad (3)$$

where λ is the X-ray wavelength of radiation used, θ is the Bragg angle, and β is the full width of the diffraction line at half maximum (FWHM) intensity measured in radians.

The content of the β-crystal was determined according to procedures described in the literatures, employing the following equation[12,42–44]:

$$k_\beta = \frac{A_{\beta(110)}}{A_{\beta(110)} + A_{\alpha(110)} + A_{\alpha(040)} + A_{\alpha(130)}} \quad (4)$$

k_β denotes the relative content of β-crystal form (WAXD), $A_{\alpha(110)}$, $A_{\alpha(040)}$, and $A_{\alpha(130)}$ are the intensities of the strongest peaks of α-form attributed to the (110), (040), and (130) planes of monoclinic cell, respectively. $A_{\beta(110)}$ is the intensity of the strongest (110) diffraction peak of the trigonal β-form.[12,13,43]

RESULTS AND DISCUSSIONS

WAXD Analysis

The virgin polymers are molded at 210°C, 10 MPa for 5 min into thin sheets of 500 μm thickness. Then, the WAXD is performed and the obtained results are shown in Figure 3 and Table I.

Table I. The Crystallite Size L and the Content of the **β**-Crystal k_β of pure PP, NPP, and WPP

Parameters	Samples	α(110)	β(110)	α(040)	α(130)
L (nm)	PurePP	18.9	-	22.4	14.9
	NPP	9.2	28.7	17.0	-
	WPP	11.0	34.0	20.5	14.1
k_β (%)	PurePP	0.0			
	NPP	83.9			
	WPP	74.8			

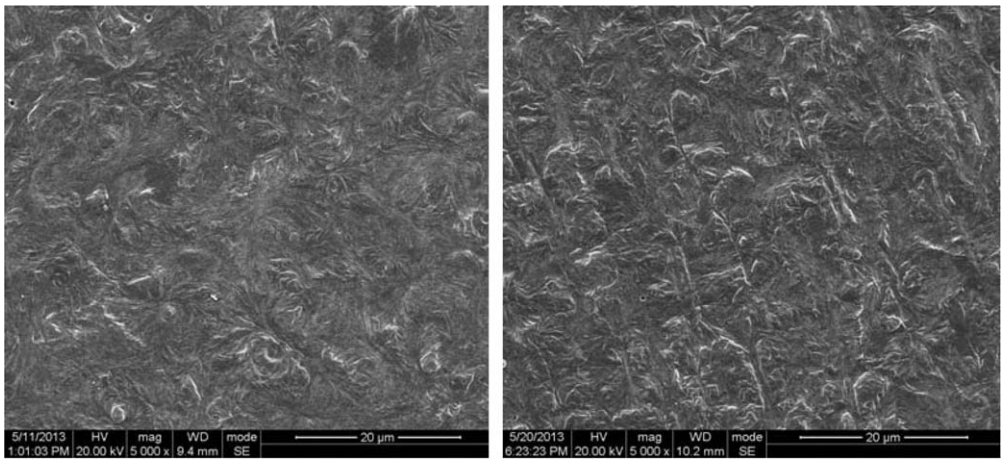

Figure 4. SEM images of the etched samples (a) NPP and (b) WPP.

As can be seen from Figure 3, for pure PP sample, only the diffraction peaks of α-phase can be observed; for NPP and WPP, besides the α-diffraction peaks, the sharp diffraction peak at $2\theta = 16.0°$, characteristic of $\beta(110)$ plane can be observed in their WAXD profiles, suggesting the formation of large amount of β-phase. Meanwhile, the intensities of planes of α-phase, α(110), α(040), and α(130), of WPP are all higher than that of NPP, indicating that more amount of α-phase has formed within WPP, namely, the selectivity of WBG-II is lower as compared with NAB83.

Table I shows that the crystallite size L decreases after the addition of WBG-II or NAB83; meanwhile, for NPP, the L of all the planes are smaller than that of WPP, indicating that the crystallite size of NPP is smaller than WPP. On the other hand, the k_β of NPP (83.9%) is higher than that of WPP (74.8%), indicating that NAB83 is more effective in inducing β-phase as compared with WPP.

SEM Observation

SEM is performed on the etched samples in order to study the morphologies of the β-PP samples. The obtained results are shown in Figure 4.

Figure 4 shows that under the same processing condition, the morphologies of NPP and WPP are quite different. NPP exhibits its typical β-spherulites morphology with face like lamellar arrangement,[33] while WPP shows an unusual morphology: many finely dispersed transcrystalline structures can be observed, and the crystals grow on the lateral surface of these dendritic structures. This interesting phenomenon can be related to the solubility of WBG-II within PP matrix and its special self-organization behavior depending on the fusion temperature applied.[22,37] Luo et al.[37] claimed that during the molding process, the WBG-II can dissolve in PP matrix to different extent, resulting different self-organization morphologies and finally induce the formation of β-PP with different morphologies (such as β-spherulites, β-transcrystalline entity, and "flower"-like agglomerate if β-crystallites). It can be concluded

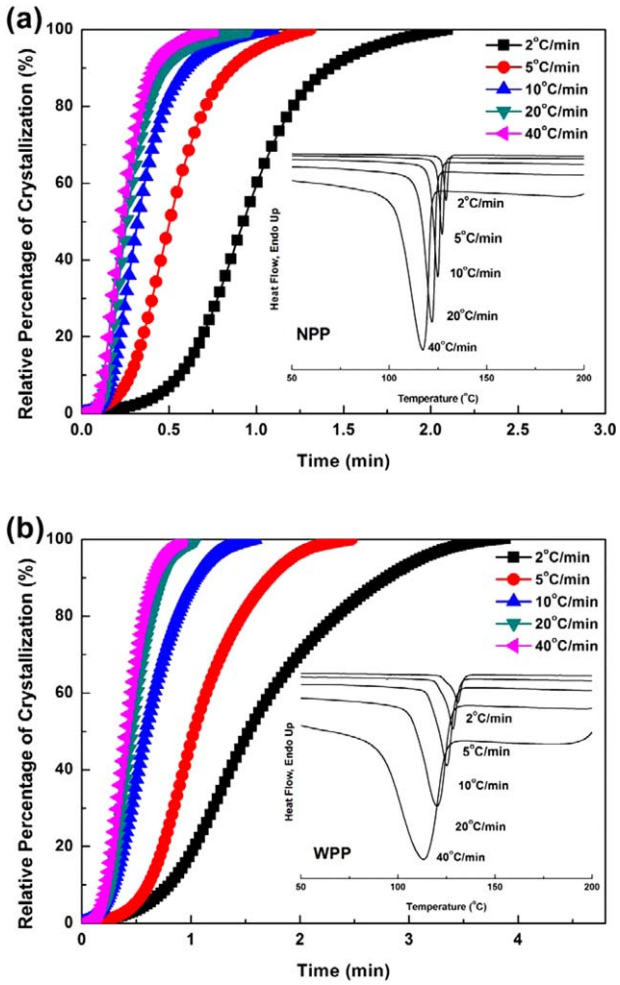

Figure 5. Plots of the relative crystallinity versus crystallization time t for (a) NPP, (b) WPP under different cooling rates. The inset gives the corresponding exothermic DSC curves. [Color figure can be viewed in the online issue, which is available at wileyonlinelibrary.com.]

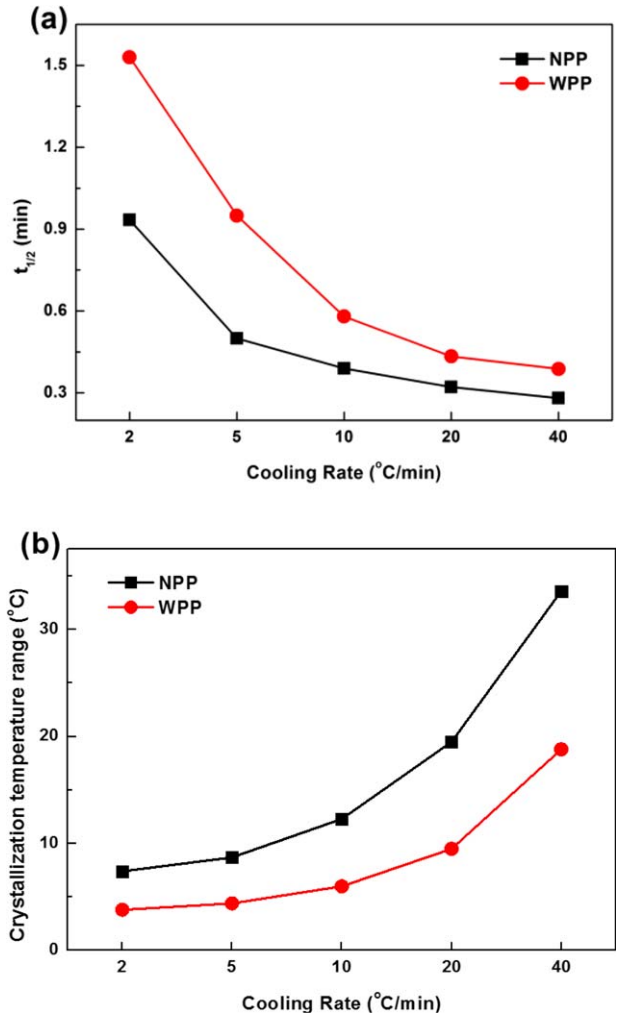

Figure 6. Crystallization parameters of the samples under different cooling rates. (a) Half-time of crystallization $t_{1/2}$ and (b) crystallization temperature range $T_{onset} - T_{endset}$. [Color figure can be viewed in the online issue, which is available at wileyonlinelibrary.com.]

in this study, the WBG-II forms tiny needles due to the self-organization behavior, and finally induces the formation of β-transcrystalline entity. In this way, the formed β-crystals exhibit special morphology as observed above.

On the other hand, few dark areas (α-phase) can be observed from the SEM image of NPP, while more dark areas can be seen from SEM image of WPP, showing that more amount of α-phase has formed in WPP, which is in accord with the results of WAXD.

Non-Isothermal Crystallization and Melting Behavior

In nonisothermal crystallization kinetics, samples are firstly cooled from the melt to 30°C at various cooling rate, 2, 5, 10, 20, and 40°C/min, then they were heated under the rate of 10°C/min to 200°C.

Crystallization Behavior

Figure 5 shows the crystallization curves of the samples at different cooling rates, and the accumulated curves of the relative

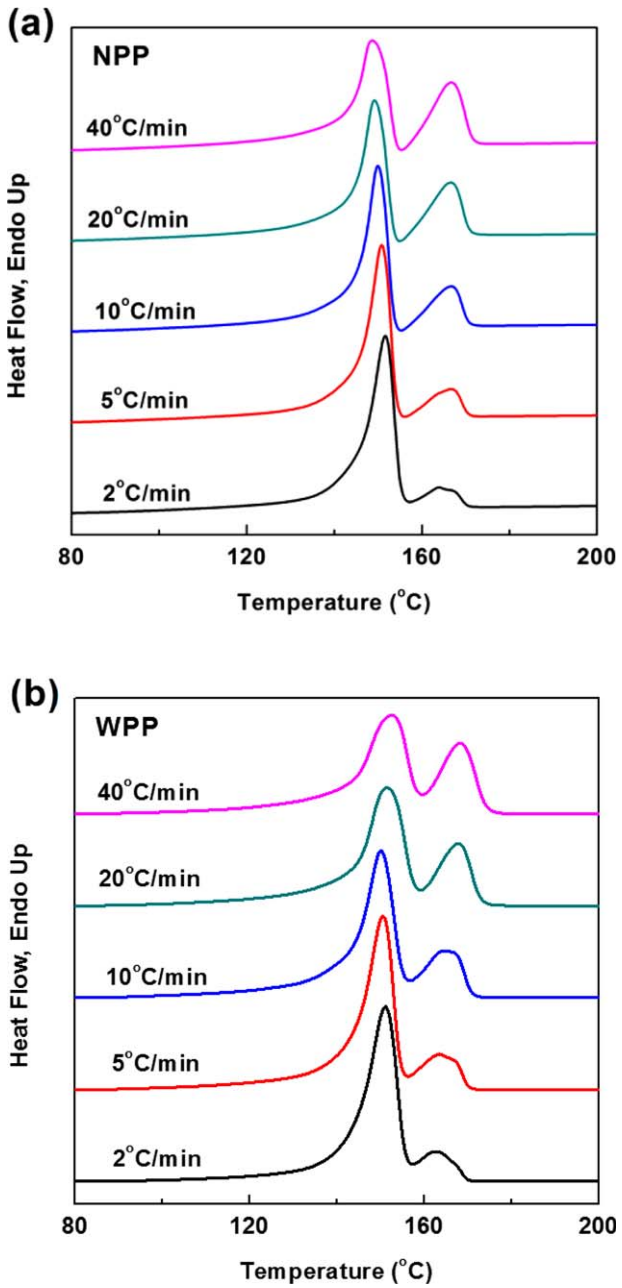

Figure 7. DSC heating thermograms of the β-iPP samples after cooled under different cooling rates (a) NPP and (b) WPP. [Color figure can be viewed in the online issue, which is available at wileyonlinelibrary.com.]

crystallinity as a function of crystallization time. From Figure 5, the half crystallization time $t_{1/2}$ and the crystallization peak width $T_{onset} - T_{endset}$ are calculated as shown in Figure 5, where the $t_{1/2}$ is defined as the half period (i.e., 50% crystallization) from the onset to endset of crystallization, which is a direct measure of crystallization rate; the crystallization peak width is denoted as the temperature width from the onset temperature to endset temperature of crystallization, which is an indicator of the crystallization temperature range.

As can be seen from Figures 5 and 6, the crystallization peak temperature of NPP and WPP decreases gradually as the cooling rate increases. Under the same cooling rate, the crystallization

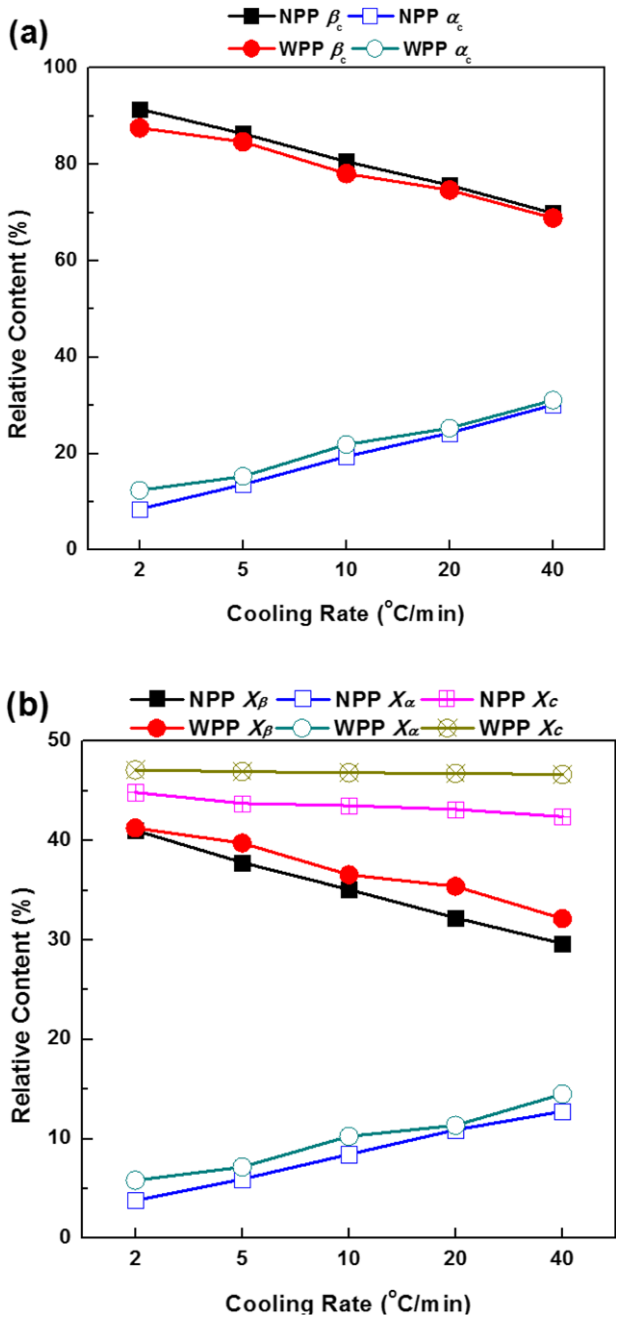

Figure 8. (a) Relative percentages of crystallinity of β-phase β_c and α-phase α_c (b) the degrees of crystallinity of β-phase X_β and α-phase X_α and relative degree of crystallinity X_c of the samples as a function of cooling rate. All the values were evaluated from heating curves in Figure 7. [Color figure can be viewed in the online issue, which is available at wileyonlinelibrary.com.]

peak width of WPP is obviously wider than that of NPP, showing that crystallization of WPP can take place at wider temperature range as compared with NAB83.

On the other hand, the half crystallization time $t_{1/2}$ of NPP is lower than that of WPP under the same cooling condition, indicating that the crystallization time of NPP is shorter than that of WPP. NAB83 can enhance the crystallization of β-PP within shorter time.

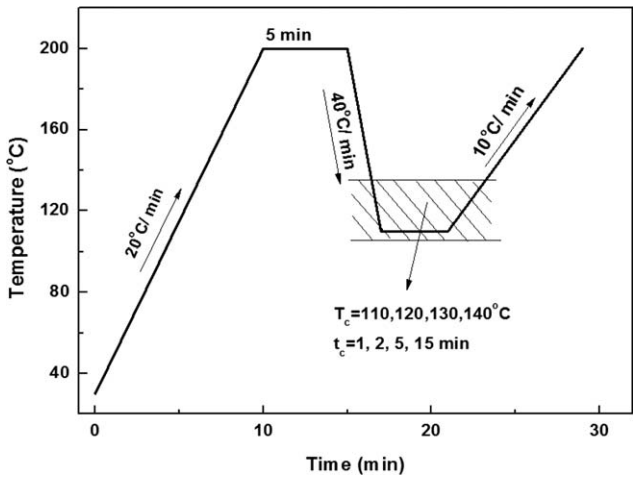

Scheme 1. Thermal protocol of the isothermal crystallization study without cooling.

Melting Behavior

The subsequent melting curves at the heating rate of 10°C/min of NPP and WPP are shown in Figure 7. According to Figure 7, the relative percentages of crystallinity of α-crystal α_c and β-crystal β_c, the degree of crystallinity of α-crystal X_α and β-crystal X_β, and the relative degree of crystallinity X_c are calculated as plotted in Figure 8.

As can be seen from Figures 7 and 8, as the cooling rate increases, the relative percentage of crystallinity of β-phase β_c, the degrees of crystallinity of β-phase X_β for both NPP and WPP decrease gradually, revealing that slow cooling rate favors the formation of high proportion of β-phase, for both NPP and WPP. Meanwhile, at the same cooling rate, NPP has higher β_c but lower X_β as compared with WPP, which can be attributed to the lower relative degree of crystallinity X_c of NPP.

It should be noted that, the heating curve of β-PP could be treated as the superposition of (1) endothermic melting curve of the β-form, (2) the exothermic crystallization curves of the molten amorphous mass crystallizing into the α-form, and (3) the final endothermic melting curve of the α-form.[45] If the thermal stability of the β-phase is lower, more fraction of molten amorphous crystallizes into the α-form, its exothermic curve will be overlapped with the melting curve of the β-form to a larger extent, resulting in a lower peak valley located between the β- and α-phase melting peak (sometimes the peak valley is even lower than the baseline of the melting curve).[7,35] Therefore, the peak valley located between the β- and α-melting peaks (at about 157°C in this study) could be used to qualitatively evaluate the thermal stability of the β-phase.[7,35,45] In Figure 7, it can be observed that for both WPP and NPP, the peak valley becomes higher as the cooling rate decreases, indicating that lower cooling rate favors the formation of β-phase with higher thermal stability. Moreover, at fixed cooling rate, the peak valley of NPP is lower than that of WPP, indicating that the thermal stability of the β-phase of NPP is lower than its counterpart of WPP. This result can also explain the difference between the results of WAXD and DSC.

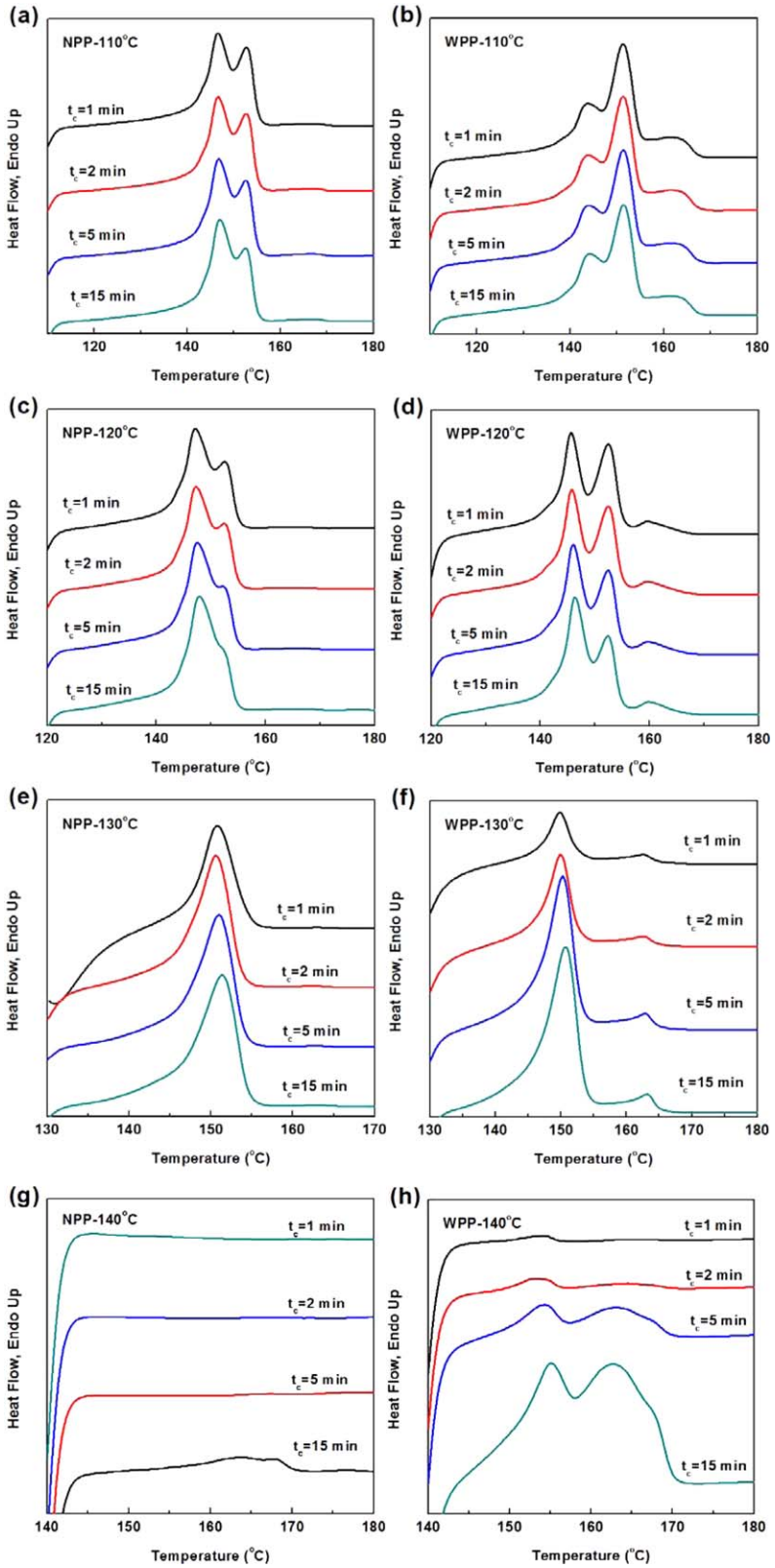

Figure 9. Melting curves of the samples after isothermally crystallized at T_c for t_c.(a, b) $T_c = 110°C$, (c,d) $T_c = 120°C$, (e–f) $T_c = 130°C$, (g,h) $T_c = 140°C$. [Color figure can be viewed in the online issue, which is available at wileyonlinelibrary.com.]

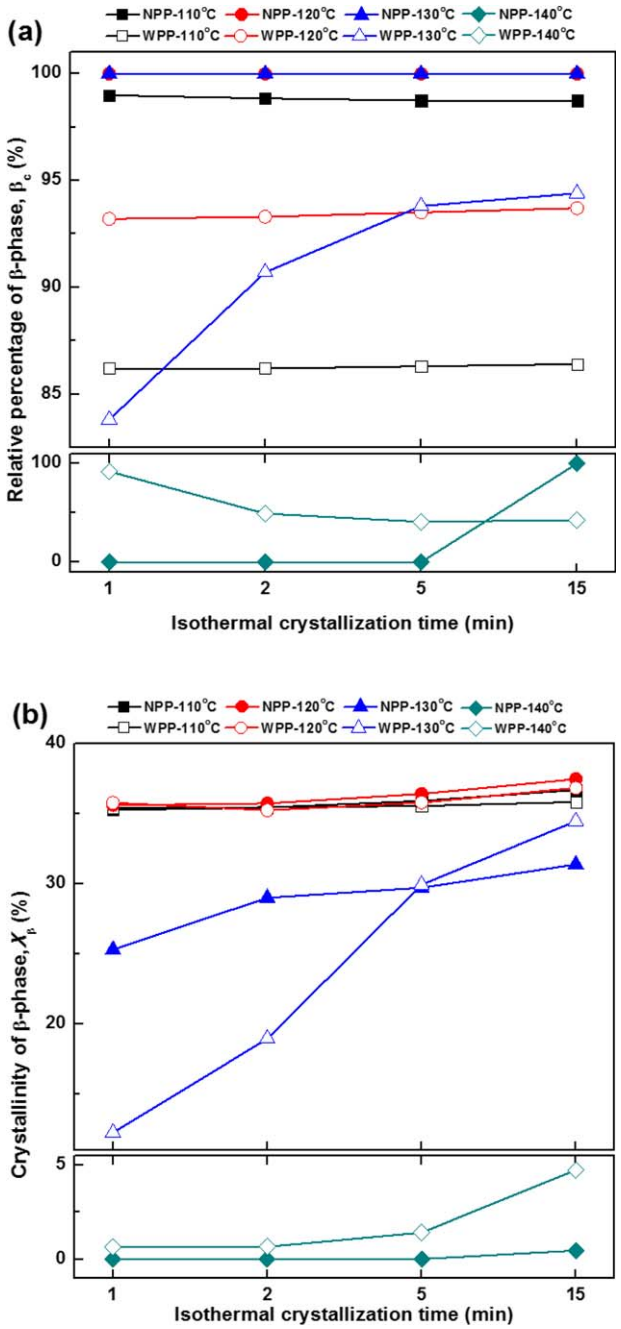

Figure 10. Melting parameters of the samples after cooled down to the isothermal crystallization temperature T_c and held for t_c. [Color figure can be viewed in the online issue, which is available at wileyonline library.com.]

Isothermal Crystallization Without Cooling

To study the effect of isothermal crystallization on the crystallization behavior of NPP and WPP, the isothermal crystallization experiment without subsequent cooling, based on DSC has performed according to the thermal protocol in Scheme 1. After erasure of the thermal history by holding the sample at 200°C for 5 min, the sample is rapidly cooled to the isothermal crystallization temperature T_c and held at this temperature for t_c.

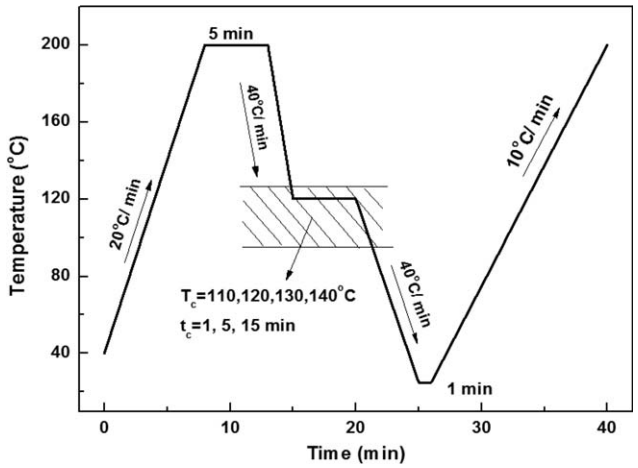

Scheme 2. Thermal protocol of the isothermal crystallization study with subsequent cooling.

After that, it is heated to 200°C at the heating rate of 10°C/ min.

The obtained melting curves of the samples are shown in Figure 9. Moreover, the relative percentages of crystallinity of α-crystal α_c and β-crystal β_c, the degree of crystallinity of α-crystal X_α and β-crystal X_β are calculated from Figure 9 and are plotted in Figure 10, as a function of crystallization time t_c.

As can be seen from Figures 9 and 10, at the isothermal crystallization temperature $T_c = 110–130$°C, the relative percentage of β-phase β_c of NPP is higher than 97%, and the crystallinity of β-phase X_β is higher than 35%, showing strong β-nucleation efficiency and high selectivity of NAB83. Meanwhile, the isothermal crystallization time t_c has little influence on the β_c and X_β, indicating that the nucleation rate of NPP is high. However, at the T_c of 140°C, NPP can hardly crystallize.

On the other hand, for WPP, when $T_c = 110$, 120°C, high proportion of β-phase with β_c higher than 85% and X_β higher than 35% has formed, indicating a strong β-nucleation efficiency of WBG-II. The fact that the β_c of WPP is lower than that of NPP reveals that, the selectivity of WBG-II is lower than NAB83. When T_c reaches 130°C, the WPP exhibits high dependence on the isothermal crystallization t_c: as the t_c increases from 1 to 15 min, the β_c increases from 83.7% to 94.4%, meanwhile, the X_β increases from 12.3% to 34.4%. This phenomenon can be explained by the relatively slow nucleation rate of WPP. At this high T_c of 130°C, longer t_c favors the formation of higher proportion of β-phase for WPP. As the t_c increases to 140°C, more amount of α- and β-phase can be observed in WPP, revealing that WBG-II can induce the formation of both α- and β-phase at this T_c, showing a wider crystallization temperature range as compared with NPP.

The above results demonstrated that, $T_c = 110$, 120°C favor the formation of high proportion of β-phase within the short t_c of 1 min for both NPP and WPP. NPP exhibits higher selectivity and higher nucleation rate in the T_c of 110°–130°, which can hardly induce the formation of β-phase when T_c reaches 140°. On the other hand, WPP has lower selectivity and lower cooling

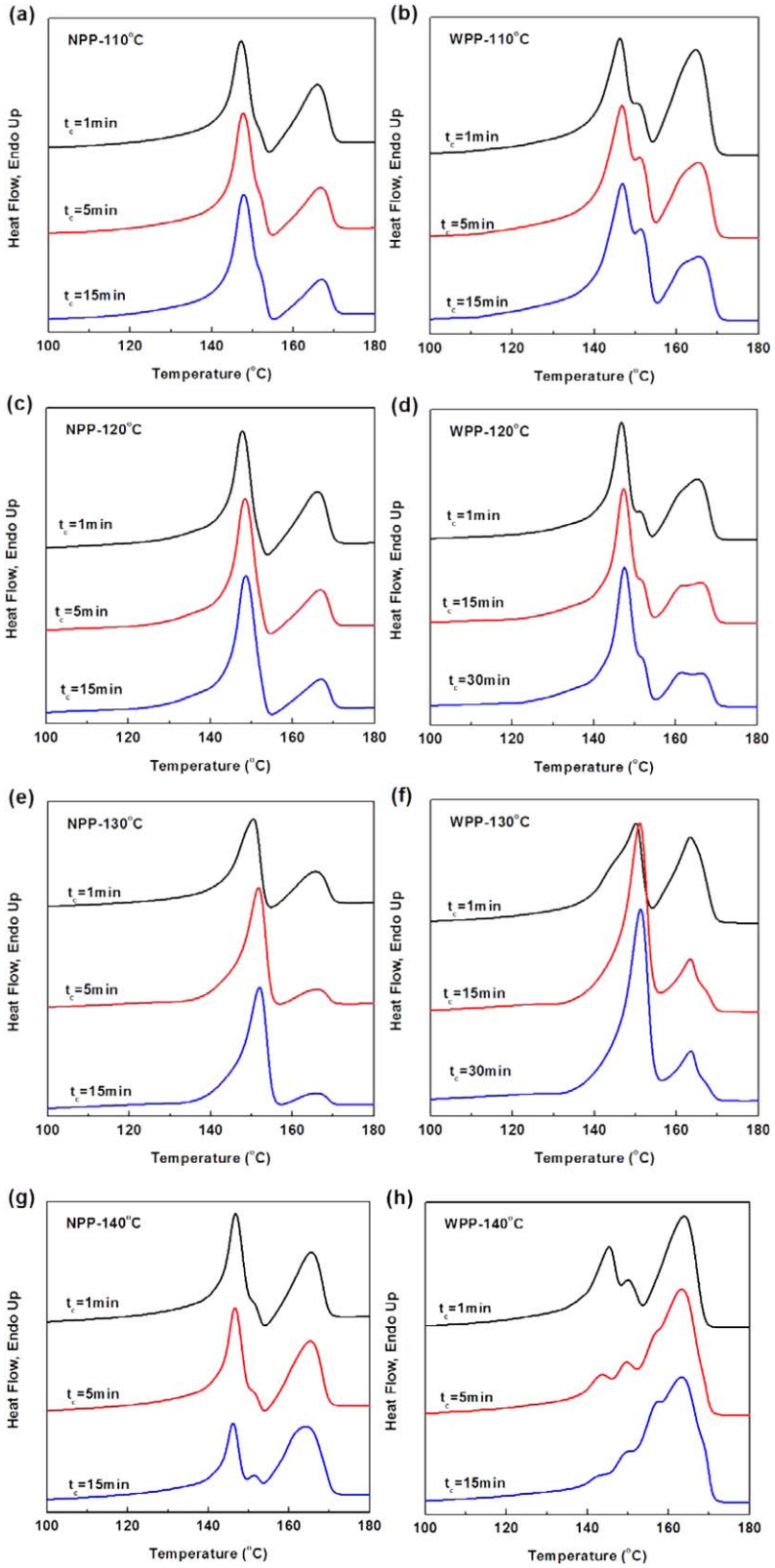

Figure 11. Melting curves of samples after isothermally crystallized at T_c for t_c and then cooled down to 40°C. (a, b) $T_c = 110$°C, (c, d) $T_c = 120$°C, (e–f) $T_c = 130$°C, (g–h) $T_c = 140$°C. [Color figure can be viewed in the online issue, which is available at wileyonlinelibrary.com.]

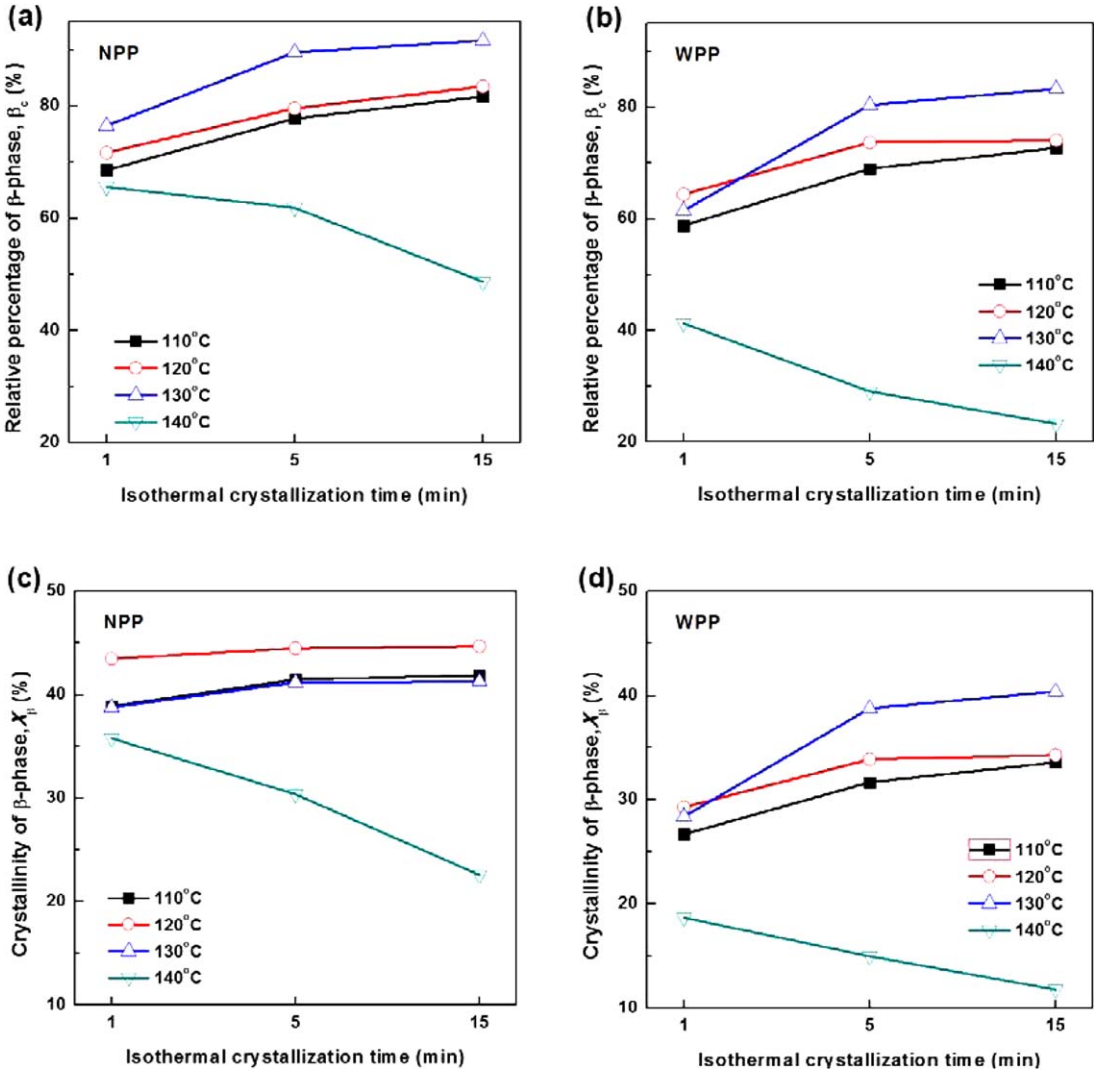

Figure 12. Melting parameters of the samples after isothermally crystallized at T_c for t_c and then cooled down to 25°C. [Color figure can be viewed in the online issue, which is available at wileyonlinelibrary.com.]

rate compared with NPP, but it can induce the crystallization in wider temperature region (even when $T_c = 140$°C in this study).

Isothermal Crystallization with Subsequent Cooling

To study the influence of subsequent cooling after isothermal crystallization on the crystallization behavior of NPP and WPP, experiments based on DSC has performed according to the thermal protocol in Scheme 2. The samples are firstly held at 200°C for 5 min to erase thermal history, and then they are rapid cooled to the isothermal crystallization temperature T_c (110, 120, 130, and 140°C) and held for t_c (1, 5, and 15 min). After that, they are cooled down to 25°C and held for 1 min to finish crystallization. Finally, they are heated at 10°C/min to 200°C. The cooling rate used is 40°C/min.

The obtained melting curves of the NPP and WPP are shown in Figure 11. The relative percentages of crystallinity of α-crystal α_c and β-crystal β_c, the degree of crystallinity of α-crystal X_α and β-crystal X_β are calculated from Figure 11 and are plotted as a function of crystallization time t_c as shown in Figure 12.

Figures 11 and 12 reveal that as the isothermal crystallization temperature increases from 110 to 130°C, the β_c of NPP and WPP increase gradually. Meanwhile, β_c also increases with the increase of isothermal crystallization temperature t_c. At the same cooling condition, NPP has higher β_c and X_c as compared with WPP, indicating that NAB83 possesses higher nucleation efficiency than that of WBG-II. On the other hand, it can be observed from Figure 12(c,d) that, within the T_c range of 110–130°C, the X_β of NPP is higher than WPP under the same crystallization condition. Meanwhile, X_β has lower sensitivity to the t_c, indicating that the nucleation rate of NPP is larger than WPP.

On the other hand, when $T_c = 140$°C, the X_β and β_c of NPP and WPP decrease significantly, which means that $T_c = 140$°C is not favorable for the formation of β-phase. Meanwhile, X_β and

β_c decrease as the t_c increases, which could be explained as follows: at the isothermal crystallization temperature of 140°C, the formation of α-phase is more favorable in thermaldynamics. As the t_c increases, more and more α-phase forms, which further leads the formation of α-phase instead of β-phase. Since WBG-II has stronger nucleation effect at high T_c and has lower selectivity compared with NAB83, more amount of α-phase has formed during the isothermal crystallization at 140°C, which restrains the subsequent β-phase nucleation.

The above results of isothermal crystallization with and without subsequent cooling to room temperature reveal that, different β-NAs have different nucleation efficiency and nucleation temperature range. NAB83 has higher selectivity and higher efficiency, which favors the formation of high proportion of β-phase at all isothermal crystallizations studied (with T_c not higher than 130°C); WBG-II higher lower selectivity, which can induce high content of β-phase under isothermal crystallization without subsequent cooling to 25°C.

CONCLUSIONS

In this study, the crystallization behavior of the β-PP samples nucleated by a rare earth based β-NA (WBG-II) and a metal salts compound β-NA (NAB83) under different cooling conditions were comparatively investigated. The studied cooling conditions include the cooling rate, isothermal crystallization temperature, isothermal crystallization time, and the subsequent cooling to room temperature. The following conclusions can be drawn.

The results of WAXD, SEM, and nonisothermal crystallization reveal that under the same processing conditions, the crystallite size of NPP is smaller, which arrange more compactly as compared with WPP. The crystalline morphologies of the samples are quite different, owning to the different self-assemble behaviors of the β-NAs. On the other hand, NPP has shorter crystallization rate and higher β-nucleation selectivity, but WPP can crystallization at wider temperature range.

The differences in selectivity, nucleation rate, and nucleation temperature of the β-NAs provide the β-PP different dependences on the isothermal crystallization conditions. NAB83 has higher selectivity and higher β-nucleation efficiency, which favors the formation of high proportion of β-phase at the isothermal crystallization temperature of 110–130°C with and without subsequent cooling; WBG-II has lower selectivity, which can only induce high content of β-phase under isothermal crystallization without subsequent cooling to 25°C. In tuning the crystallization behavior and the properties of β-PP, the joint influence of the efficiency and selectivity of the β-NA, and the thermal conditions (such as cooling rates, isothermal crystallization temperature and time, and the subsequent cooling to room temperature) should be taken into consideration.

ACKNOWLEDGMENTS

The authors express their sincerely thanks to the Sichuan University Scientific Research Foundation for Young Teachers (2012SCU11075) and National Science Foundation of China (NSFC 51203106).

REFERENCES

1. Busico, V.; Cipullo, R. *Prog. Polym. Sci.* **2001**, *26*, 443.
2. Kang, J.; Cao, Y.; Li, H.; Li, J.; Chen, S.; Yang, F.; Xiang, M. *J. Polym. Res.* **2012**, *19*, 37.
3. Zhu, L.; Cao, J.; Wang, Y. *J. Appl. Polym. Sci.* **2013**, *129*, 1520.
4. Kang, J.; Yang, F.; Wu, T.; Li, H.; Cao, Y.; Xiang, M. *Eur. Polym. J.* **2012**, *48*, 425.
5. Kang, J.; Li, J.; Chen, S.; Zhu, S.; Li, H.; Cao, Y.; Yang, F.; Xiang, M. *J. Appl. Polym. Sci.* **2013**, *130*, 25.
6. Horvath, S. I.; Stoll, Z.; Varga, J. eXPRESS Polym. *Lett.* **2010**, *4*, 101.
7. Kang, J.; Gai, J.; Li, J.; Chen, S.; Peng, H.; Wang, B.; Cao, Y.; Li, H.; Chen, J.; Yang, F.; Xiang, M. *J. Polym. Res.* **2013**, *20*, 70.
8. Kang, J.; Chen, J.; Cao, Y.; Li, H. *Polymer* **2010**, *51*, 249.
9. Li, X.; Wu, H.; Chen, J.; Yang, J.; Huang, T.; Zhang, N.; Wang, Y. *J. Appl. Polym. Sci.* **2012**, *126*, 1031.
10. Natta, G.; Corradini, P. *Il Nuovo Cimento Series 10* **1960**, *15*, 40.
11. Lotz, B. *Eur. Phys. J. E* **2000**, *3*, 185.
12. Dorset, D. L.; McCourt, M. P.; Kopp, S.; Schumacher, M.; Okihara, T.; Lotz, B. *Polymer* **1998**, *39*, 6331.
13. Mathieu, C.; Thierry, A.; Wittmann, J. C.; Lotz, B. *J. Polym. Sci. Part B: Polym. Phys.* **2002**, *40*, 2504.
14. Meille, S. V.; Ferro, D. R.; Brueckner, S.; Lovinger, A. J.; Padden, F. *J. Macromolecules* **1994**, *27*, 2615.
15. Meille, S.; Bruckner, S. *Nature* **1989**, *340*, 455.
16. Bruckner, S.; Phillips, P. J.; Mezghani, K.; Meille, S. V. *Macromol. Rapid. Commun.* **1997**, *18*, 1.
17. Bruckner, S.; Meille, S. V.; Petraccone, V.; Pirozzi, B. *Prog. Polym. Sci.* **1991**, *16*, 361.
18. Li, H.; Jiang, S.; Wang, J.; Wang, D.; Yan, S. *Macromolecules* **2003**, *36*, 2802.
19. Xiao, W.; Wu, P.; Feng, J. *J. Appl. Polym. Sci.* **2008**, *108*, 3370.
20. Xiao, W.; Wu, P.; Feng J.; Yao, R. *J. Appl. Polym. Sci.* **2009**, *111*, 1076.
21. Wang, S.; Yang, W.; Xu, Y.; Xie, B.; Yang, M.; Peng, X. *Polym. Test.* **2008**, *27*, 638.
22. Luo, F.; Geng, C.; Wang, K.; Deng, H.; Chen, F.; Fu, Q.; Na, B. *Macromolecules* **2009**, *42*, 9325.
23. Yu, T.; Wu, C.; Wang, C.; Rwei, S. *Compos. Interfaces* **2013**, *20*, 483.
24. Dong, M.; Guo, Z.; Su, Z.; Yu, J. *J. Appl. Polym. Sci.* **2011**, *119*, 1374.
25. Bai, H.; Luo, F.; Zhou, T.; Deng, H.; Wang, K.; Fu, Q. *Polymer* **2011**, *52*, 2351.
26. Xiao, W.; Wu, P.; Feng, J.; Yao, R. *J. Appl. Polym. Sci.* **2009**, *111*, 1076.
27. Grein, C. *Adv. Polym. Sci.* **2005**, *188*, 43.
28. Chvatalova, L.; Navratilova, J.; Cermak, R.; Raab, M.; Obadal, M. *Macromolecules* **2009**, *42*, 7413.

29. Cai, Z.; Li, J.; Shang, Y.; Huo, H.; Feng, J.; Funari, S.; Jiang, S. *J. Appl. Polym. Sci.* **2013**, *128*, 628.
30. Zhang, B.; Chen, J.; Ji, F.; Zhang, X.; Zheng, G.; Shen, C. *Polymer* **2012**, *53*, 1791.
31. Cai, Z.; Zhang, Y.; Li, J.; Xue, F.; Shang, Y.; He, X.; Feng, J.; Wu, Z.; Jiang, S. *Polymer* **2012**, *53*, 1593.
32. Yuan, Q.; Jiang, W.; An, L. *Colloid Polym. Sci.* **2004**, *282*, 1236.
33. Ran, S.; Xu, M. *Chin. J. Polym. Sci.* **2004**, *22*, 123.
34. Chu, F.; Ide, H.; Kimura, Y. *Polymer* **1994**, *35*, 3442.
35. Varga, J. *J. Macromol. Sci. Part B* **2002**, *41*, 1121.
36. Chu, F.; Kimura, Y. *Polymer* **1996**, *37*, 573.
37. Luo, F.; Wang, K.; Ning, N.; Geng, C.; Deng, H.; Chen, F.; Fu, Q.; Qian, Y.; Zheng, D. *Polym. Adv. Technol.* **2011**, *22*, 2044.
38. Luo, F.; Geng, C.; Wang, K.; Deng, H.; Chen, F.; Fu, Q.; Na, B. *Macromolecules* **2009**, *42*, 9325.
39. Kang, J.; Li, J.; Chen, S.; Peng, H.; Wang, B.; Cao, Y.; Li, H.; Chen, J.; Gai, J.; Yang, F.; Xiang, M. *J. Appl. Polym. Sci.* **2013**, *129*, 2663.
40. Olley, R. H.; Bassett, D. C.; Blundell, D. *J. Polymer* **1986**, *27*, 344.
41. Luo, F.; Wang, J.; Bai, H.; Wang, K.; Deng, H.; Zhang, Q.; Chen, F.; Fu, Q.; Na, B. *Mater. Sci. Eng. A: Struct.* **2011**, *528*, 7052.
42. Turner-Jones, A.; Aizlewood, J.; Beckett, D. *Makromol. Chem.* **1964**, *75*, 134.
43. Ferro, D. R.; Meille, S. V.; Bruckner, S. *Macromolecules* **1998**, *31*, 6926.
44. Mao, Y.; Li, X.; Burger, C.; Hsiao, B.; Tsou, A. *Polymer* **2013**, *54*, 1432.
45. Yamamoto, Y.; Inoue, Y.; Onai, T.; Doshu, C.; Takahashi, H.; Uehara, H. *Macromolecules* **2007**, *40*, 2745.